Long non-coding RNA Meg3 deficiency impairs glucose homeostasis and insulin signaling by inducing cellular senescence of hepatic endothelium in obesity

Authors: Xiao Cheng[a,1], Mohamed Sham Shihabudeen Haider Ali[a,1], Matthew Moran[a], Martonio Ponte Viana[a], Sarah L. Schlichte[b], Matthew C. Zimmerman[b,c], Oleh Khalimonchuk[a,c,d], Mark W. Feinberg[e], Xinghui Sun[a,d,f,2]

Affiliations:

[a] Department of Biochemistry, University of Nebraska - Lincoln, Beadle Center, 1901 Vine St, Lincoln, Nebraska 68588, USA;

[b] Department of Cellular and Integrative Physiology, University of Nebraska Medical Center, 985850 Nebraska Medical Center, Omaha, Nebraska 68198-5850, USA;

[c] Nebraska Redox Biology Center, University of Nebraska – Lincoln;

[d] Nebraska Center for Integrated Biomolecular Communication, University of Nebraska – Lincoln;

[e] Cardiovascular Division, Department of Medicine, Brigham and Women's Hospital, Harvard Medical School, Boston, Massachusetts, USA;

[f] Nebraska Center for the Prevention of Obesity Diseases through Dietary Molecules, University of Nebraska - Lincoln.

[1] X.C. and M.S.S. contributed equally to this work.

[2] To whom correspondence may be addressed: Dr. Xinghui Sun, Department of Biochemistry, Beadle N158, University of Nebraska – Lincoln, 1901 Vine Street, Lincoln, NE 68588-0665, USA.

Tel: [+1 402 472 8898], Fax: [+1 402 472 7842], Email: xsun17@unl.edu

Materials and Methods

Proteomic analysis using TMT10-plex labeling and liquid chromatography-tandem mass spectrometry (LC-MS/MS)

Proteomics experiments in Fig. S6 were carried out by the Proteomics and Mass Spectrometry Core facility at Princeton University. Frozen liver tissues were washed with 500 µl of 50 mM ammonium bicarbonate buffer and transferred to low binding Eppendorf tube. Then 100 µl of lysis buffer (6 M guanidine Hydrochloride, 10 mM TCEP, 40 mM CAA, 100 mM Tris pH 8.5, 1x MS-Safe protease inhibitor, 1x Phosphatase inhibitor cocktail II) was added and liver tissues were smashed with pellet pestle. Samples were vortexed and heated to 95 °C for 10 min with Thermomixer (Eppendorf Co.), sonicated for 5 times (15 seconds ON / 10 seconds OFF each time), heated at 95 °C for 5 min and then spin down for 1 min at 4000 rpm. Additional 400 µl of lysis buffer was added again and the above tissue smashing with pellet pestle step to spinning down for 1 min at 4000 rpm step were performed again. Take 100 µl of supernatant and diluted 1:3 with digestion buffer (10% Acetonitrile, 25 mM Tris pH8.5) containing LysC (2 µg) and incubated at 37 °C for 3 hours. Samples were then further diluted to 1:10 with digestion buffer containing Trypsin (10 µg Sequencing Grade, Promega) and incubated overnight at 37 °C. Add 10% TFA to samples to yield final concentration of 1% TFA. Vortex and spin down for 1 min at 4000 rpm. Supernatant was collected and then desalted on C18 cartridges (Oasis, Waters) as per manufacture protocol. Desalted samples were frozen with liquid nitrogen and lyophilized. Dried peptides were reconstituted using 2 ml of 5% Acetonitrile with 0.1% formic acid. The absorbance at 205 nm was used to calculate the peptide concentration on a Nanodrop (Thermo). An aliquot of 80 µg of each sample was dried in a SpeedVac. Each sample was then reconstituted in 80 µl of 0.1 M TEAB pH 8.0 in 20% ACN. 10 µl of TMT labeling reagent was then added to each sample and incubated for 1hr at RT on a thermomixer. The reaction was quenched by adding hydroxylamine to 0.33%. The 10 samples were mixed in equimolar amounts (10 µl each) and desalted using C8-stage tips (1 x 10 gauge needle disc and 40 µl of 50% AQ3 resin slurry in methanol as in [1]). Dried peptide mix was reconstituted in 5% ACN 0.1% formic acid. The 10-plex peptide mix was then fractionated using SCX stage-tips (3 x 10 gauge needle discs) as in [2]. Six 80 µl fractions were collected using: 0.05 M ammonium acetate in 20% acetonitrile; 0.075 M ammonium acetate in 20% acetonitrile, 0.125 M ammonium acetate in 20% acetonitrile, 0.2 M ammonium acetate in 20% acetonitrile, 0.30 M ammonium acetate in 20% acetonitrile and 5% ammonium hydroxide in 80% acetonitrile. SCX fractions were dried down in SpeedVac and re-dissolved in 20 µl 5% acetonitrile with 0.1% formic acid in water. The absorbance at 205 nm was used to calculate the peptide concentration on a Nanodrop (Thermo). Another set of 10 samples were mixed in equimolar amounts (10 µl each) and eluted into eight 80 µl fractions using C8-stage tips (1 x 10 gauge needle disc and 40 µl of 50% AQ3 resin slurry in methanol as in [1]): 5% buffer B (0.1% formic acid in 80% acetonitrile), 7.5% buffer B (0.1% formic acid in 80% acetonitrile), 10% buffer B (0.1% formic acid in 80% acetonitrile), 12.5% buffer B (0.1% formic acid in 80% acetonitrile), 15% buffer B (0.1% formic acid in 80% acetonitrile), 17.5% buffer B (0.1% formic acid in 80% acetonitrile), 20% buffer B (0.1% formic acid in 80% acetonitrile), 50% buffer B (0.1% formic acid in 80% acetonitrile). C8-AQ3 fractions were dried down in

SpeedVac and re-dissolved in 20 µl 5% acetonitrile with 0.1% formic acid in water. The absorbance at 205 nm was used to calculate the peptide concentration on a Nanodrop (Thermo). C8-AQ3 fractions were pooled in the following fashion yielding 4 fractions: #1 and #5, #2 and #6, #3 and #7, #4 and #8. This resulted in 6 SCX fractions and 4 C8-AQ3 fractions with a total of 10 fractions for LC/MS/MS analysis.

Each of the 10 fractions was injected 2 µl per run using an Easy-nLC 1200 UPLC system. Samples were loaded directly onto a 45 cm long 75 µm inner diameter nano capillary column packed with 1.9 µm C18-AQ (Dr. Maisch, Germany) mated to metal emitter in-line with an Fusion Lumos (Thermo Scientific, USA). Samples were eluted using a gradient of 10-20% B (80% acetonitrile with 0.1% FA) in 32 min and 20-40% B in 92 min followed by column wash at 100% B for 10 min. The mass spectrometer was operated in data dependent mode with the 60,000 resolution MS1 scan (380-1500 m/z), AGC target of 4e5 and max injection time of 50 ms. Peptides above threshold 5e3 and charges 2-7 were selected for fragmentation with dynamic exclusion after 1 time for 60 s and 10 ppm tolerance. MS2 isolation was achieved with 0.8 m/z window by the quadruple with 0.2 m/z offset. HCD collision at 33% stepped by 5% was carried out and fragments detected by the ion trap in rapid mode with AGC target of 1e4 and max injection time of 50 ms. 10 SPS precursor were selected within 400-1200 m/z. For MS3 scan, MS1 isolation windows of 1.6m/z, MS2 isolation windows 2 and HCD NCE of 55% were selected. MS3 fragments were detected in the Orbitrap at 50,000 resolution in the mass range of 120-500 with AGC 5e4 and max injection time of 86ms. Total duty cycle was set to 3.0s.

Raw files were searched with MaxQuant (ver 1.6.0.16)[3], using default setting for MS3 reporter TMT 10-plex data. Carbamidomethylation of cysteine was used as fixed modification, oxidation of methionine, and acetylation of protein N-termini were specified as dynamic modifications. Trypsin digestion with maximum of 2 missed cleavages were allowed. Raw files were searched against mouse protein database downloaded from UniProt and supplemented with common contaminant proteins. Raw files were also analyzed within the Proteome Discoverer (v 2.1.0.81 Thermo) using Byonic [4] search node (Protein Metrics, USA). Deamidation of asparagine, oxidation of methionine, Gln->pyro-Glu of glutamine and acetylation of protein N-termini were specified in Byonic as variable modifications.

Data from Maxquant and Proteome Discoverer were combined in Scaffold Q+ (version Scaffold_4.8.4, Proteome Software Inc., Portland, OR). Scaffold was used to validate MS/MS based peptide and protein identifications. Peptide identifications were accepted if they could be established at greater than 80.0% probability by the Scaffold Local FDR algorithm. Protein identifications were accepted if they could be established at greater than 96.0% probability and contained at least 2 identified peptides. Protein probabilities were assigned by the Protein Prophet algorithm [5]. Proteins that contained similar peptides and could not be differentiated based on MS/MS analysis alone were grouped to satisfy the principles of parsimony. Scaffold Q+ unnormalized data was exported as a data table and further analyzed. Differentially expressed proteins were identified using 20% change and $P < 0.05$. Genes encoding the differentially expressed proteins were input into the Database for Annotation, Visualization and Integrated Discovery (DAVID v6.8; https://david.ncifcrf.gov/) for Gene Ontology (GO) term enrichment analysis ($P < 0.05$; at least 5 genes in a GO regulated by Meg3). The dot plot for the GO terms as the function

of enrichment scores were generated using the R package gplot. Dot sizes represent gene ratio, and colors represent *P* Values.

In situ RNA detection

Paraffin sections of human and mouse white adipose tissues were prepared for Meg3 detection. *In situ* RNA detection was performed using RNAscope® 2.5 HD Reagent Kit-RED (Advanced Cell Diagnostics) and RNAscope® Probe following the manufacturer's instructions.

Metabolic cage studies

Metabolic cage studies were performed by the Biomedical and Obesity Research Core of UNL. Room temperature for all metabolic studies was maintained at 22°C with a 12 hr light/dark cycle. Obese mice treated with gapmeRs (see the section "Mice" above). Mice were allowed to acclimate for 1 week in TSE Systems Phenomaster cages. Mice are acclimated in acclimation cages that are similar to the experimental cages, one mouse per cage. Computer controlled monitoring systems were used to investigate full metabolic profile on live mice. The heat production, indirect calorimetry (O_2 consumption and CO_2 production), food intake, as well as locomotor activity were measured. All of the parameters are measured continuously and simultaneously. Data were collected over the course of 3 days after a two-day adaptation.

Assessment of mitochondrial bioenergetics

For extracellular acidification rate (ECAR, a proxy to glycolytic flux), cell culture media were changed to modified XF assay medium containing 2 mM glutamine. After 1 h incubation at 37 ºC without CO_2, ECAR were measured using glycolysis stress test kit. The data were expressed by normalizing with protein concentration.

Supplementary figure legends

Fig. S1. *In situ* hybridization of Meg3 using RNAscope® Technology in mouse and human white adipose tissues. Representative images of *in situ* hybridization show Meg3 in red. CD31 staining (green) were examined on the adjacent sections. Nuclei was stained with DAPI in blue.

Fig. S2. Meg3 knockdown (KD) doesn't affect glycolysis in HUVECs. Extracellular acidification rate (ECAR) was examined in HUVECs transfected with control gapmeRs (Ctl) or Meg3 gapmeRs (Meg3 KD), n = 3 independent experiments.

Fig. S3. Mitochondrial (mito.) morphology quantification using a custom-modified NIH ImageJ macro. HUVECs were stained with 500 nM mitoTracker green for 30 min and treated with 10 μM FCCP for 10 min for live cell imaging (5% CO_2 and 37°C with humidity). Data were from 20 cells in each condition. Form factor = Perimeter^2/(4×Pi×area); lower values represent more fragmented mitochondria.

Fig. S4. Metabolic cage studies. Meg3 knockdown (KD) does not affect food intake (A), body weight (B), activities (C), heat (D), CO_2 production (E), or oxygen consumption (F) in obese mice. Mean ± SEM, n = 6 mice per group.

Fig. S5. Meg3 knockdown (KD) reduces the levels of phosphorylated insulin receptor β subunit (IRβ) at Tyr1150/1151. C57BL/6 mice were fed a HFD. At Week 5 on HFD, mice were intravenously injected with control gapmeRs or Meg3 gapmeRs once a week and maintained on HFD up to 12 weeks. Total insulin receptor β and the phosphorylation at Tyr1150/1151 were examined by western blot in the livers of overnight-fasted mice. The tissues were collected at 10 min after insulin injection (0.75 units/kg). Values are mean ± SEM, n = 4 per group; *, $P < 0.05$.

Fig. S6. Meg3 knockdown (KD) does not increase systemic inflammation in obese mice. (A-F) C57BL/6 mice were fed on a HFD and treated with control gapmeRs or Meg3 gapmeRs (n = 6 or 7 mice per group). **(A)** Immunofluorescence staining of Mac2 (macrophage marker) and perilipin (adipocyte marker) on eWATs sections and Mac2 quantification. **(B)** The expression of inflammatory genes was examined in eWATs by qPCR. **(C)** Immunofluorescence staining and quantification of CD68 (macrophage marker) on liver sections. **(D)** The expression of CD68 and F4/80 (macrophage markers) and MCP1 (chemokine) was examined in livers by qPCR. **(E)** The levels of plasma TNFα and MCP1 were analyzed by ELISA. **(F)** Plasma levels of ALT and AST were examined in mice treated with control gapmeRs or Meg3 gapmeRs. **(G)** Meg3 knockdown induces type I interferon response in hepatic endothelium (n=6 or 7) and in HUVECs (n=3). For all panels, values are mean ± SEM; *, $P < 0.05$.

Fig. S7. The top ten GO terms that regulated by Meg3. Livers of obese mice injected with control gapmeRs or Meg3 gapmeRs (Meg3 KD) were subjected to quantitative proteomics (TMT10plex labeling and mass spectrometry) and bioinformatics analysis of genes encoding differentially expressed proteins.

Fig. S8. p53 and Meg3 expression in the freshly isolated ECs or in the indicated tissues by qPCR or western blot. (A) p53 expression was examined in the freshly isolated ECs of livers and skeletal muscles (SM) by qPCR (n = 5 for p53 floxed mice; n=14 for p53 iECKO mice). **(B)** p53 expression was examined in the freshly isolated liver ECs by western blot. ECs were pooled from three mice each group. **(C)** The expression of CDKN1A was examined in the freshly isolated liver ECs by qPCR (n = 5, 5, 14, 14 for each group of the indicated mice, respectively). N.S., non-significant. **(D)** p53 expression was examined in the livers and skeletal muscles (SM) tissues by qPCR (n = 5 for p53 floxed mice; n=14 for p53 iECKO mice). **(E)** Meg3 expression was examined in the freshly isolated ECs of livers and skeletal muscles (SM) of p53 iECKO mice or in livers and skeletal muscles tissues of p53 iECKO mice (n=7 per group). For all panels, values are mean ± SEM; *, $P < 0.05$.

Fig. S9. Meg3 knockdown (KD) reduces the levels of phosphorylated insulin receptor β (IRβ) subunit at Tyr1150/1151. p53 floxed mice were fed a HFD. At Week 5 on HFD, mice were intravenously injected with control gapmeRs or Meg3 gapmeRs once

a week and maintained on HFD up to 12 weeks. Total insulin receptor β and the phosphorylation at Tyr1150/1151 were examined by western blot in the livers of overnight-fasted mice. The tissues were collected at 10 min after insulin injection (0.75 units/kg). Values are mean ± SEM, n = 8-12 per group; *, $P < 0.05$.

Supplementary table legends

Supplementary Table 1: Primers used in the study. “h” is the abbreviation for human; “m” is the abbreviation for mouse; “F” stands for forward, and “R” stands for reverse.

Supplementary Table 2: Demographics of human liver specimens.

Supplementary Table 3: Differentially expressed proteins in mouse livers identified by quantitative proteomics. Obese mice were injected with control gapmeRs or Meg3 gapmeRs (10 mg/kg, three injections on three consecutive days). Livers were collected at 72 hours after the last injection for TMT10-plex labelling and mass spectrometry.

References

1. Rappsilber J, Ishihama Y and Mann M. Stop and go extraction tips for matrix-assisted laser desorption/ionization, nanoelectrospray, and LC/MS sample pretreatment in proteomics. *Anal Chem*. 2003;75:663-70.
2. Kulak NA, Pichler G, Paron I, Nagaraj N and Mann M. Minimal, encapsulated proteomic-sample processing applied to copy-number estimation in eukaryotic cells. *Nat Methods*. 2014;11:319-24.
3. Cox J and Mann M. MaxQuant enables high peptide identification rates, individualized p.p.b.-range mass accuracies and proteome-wide protein quantification. *Nat Biotechnol*. 2008;26:1367-72.
4. Bern M, Kil YJ and Becker C. Byonic: advanced peptide and protein identification software. *Curr Protoc Bioinformatics*. 2012;Chapter 13:Unit13 20.
5. Nesvizhskii AI, Keller A, Kolker E and Aebersold R. A statistical model for identifying proteins by tandem mass spectrometry. *Anal Chem*. 2003;75:4646-58.

Figure S1

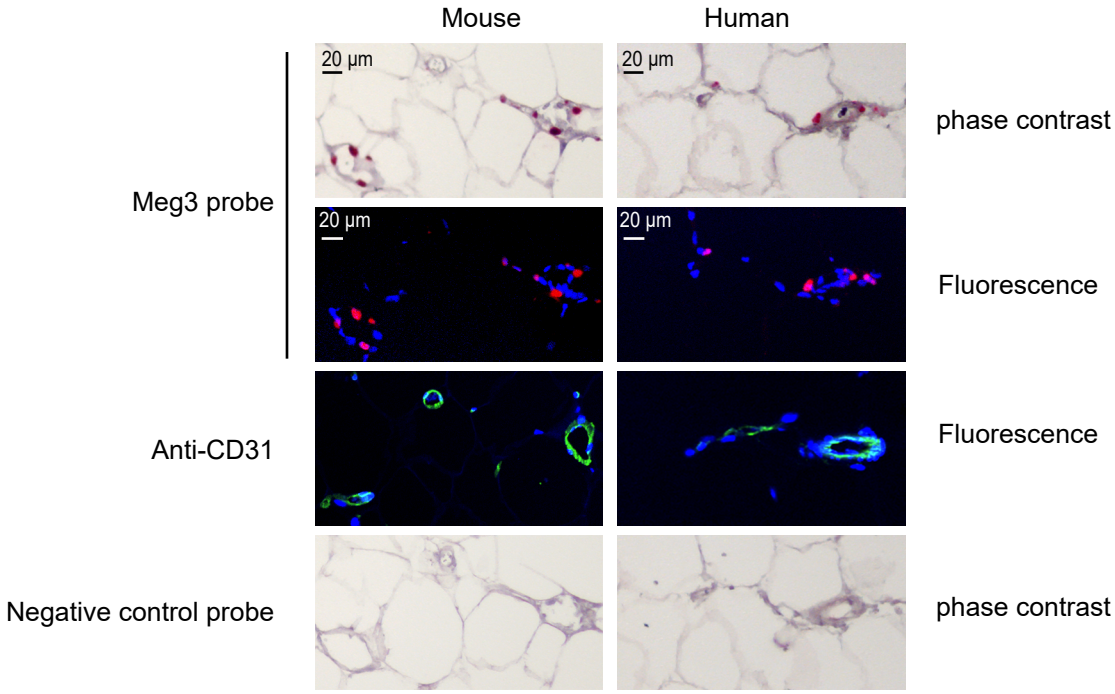

Fig. S1. *In situ* hybridization of Meg3 using RNAscope® Technology in mouse and human white adipose tissues. Representative images of *in situ* hybridization show Meg3 in red. CD31 staining (green) were examined on the adjacent sections. Nuclei was stained with DAPI in blue.

Figure S2

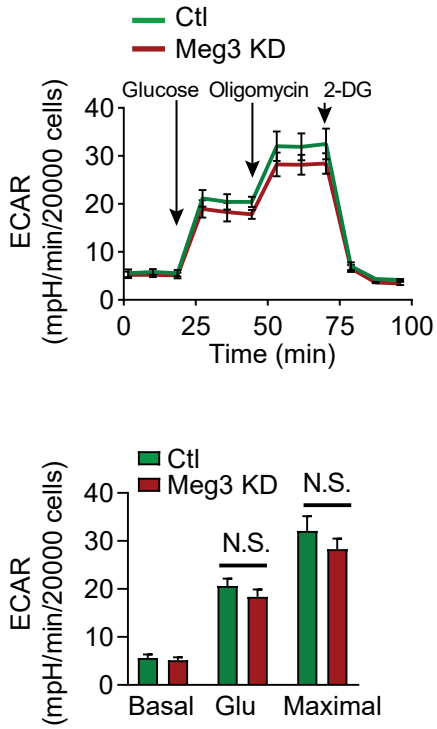

Fig. S2. Meg3 knockdown (KD) doesn't affect glycolysis in HUVECs. Extracellular acidification rate (ECAR) was examined in HUVECs transfected with control gapmeRs (Ctl) or Meg3 gapmeRs (Meg3 KD), n = 3 independent experiments. N.S., non-significant.

Figure S3

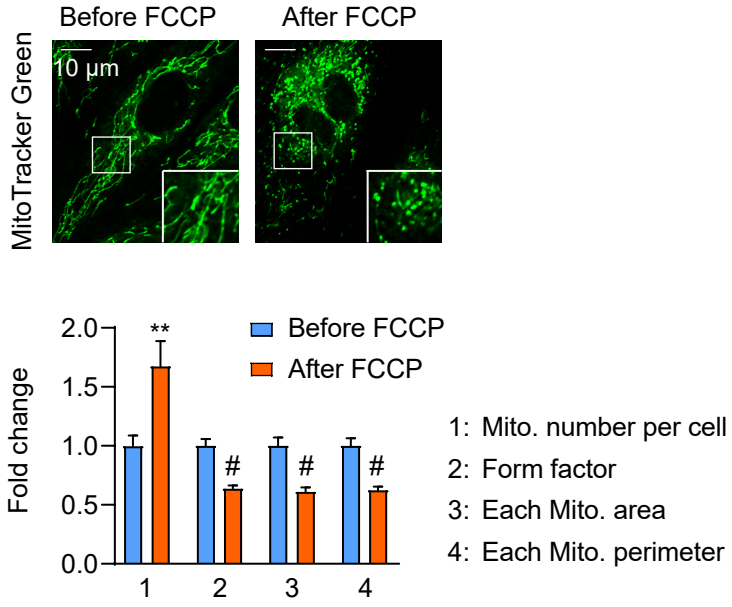

Fig. S3. Mitochondrial (mito.) morphology quantification using a custom-modified NIH ImageJ macro. HUVECs were stained with 500 nM mitoTracker green for 30 minutes and treated with 10 μM FCCP for 10 minutes for live cell imaging (5% CO2 and 37°C with humidity). Data were from 20 cells in each condition. Form factor = Perimeter^2/(4×Pi×area); lower values represent more fragmented mitochondria.

Figure S4

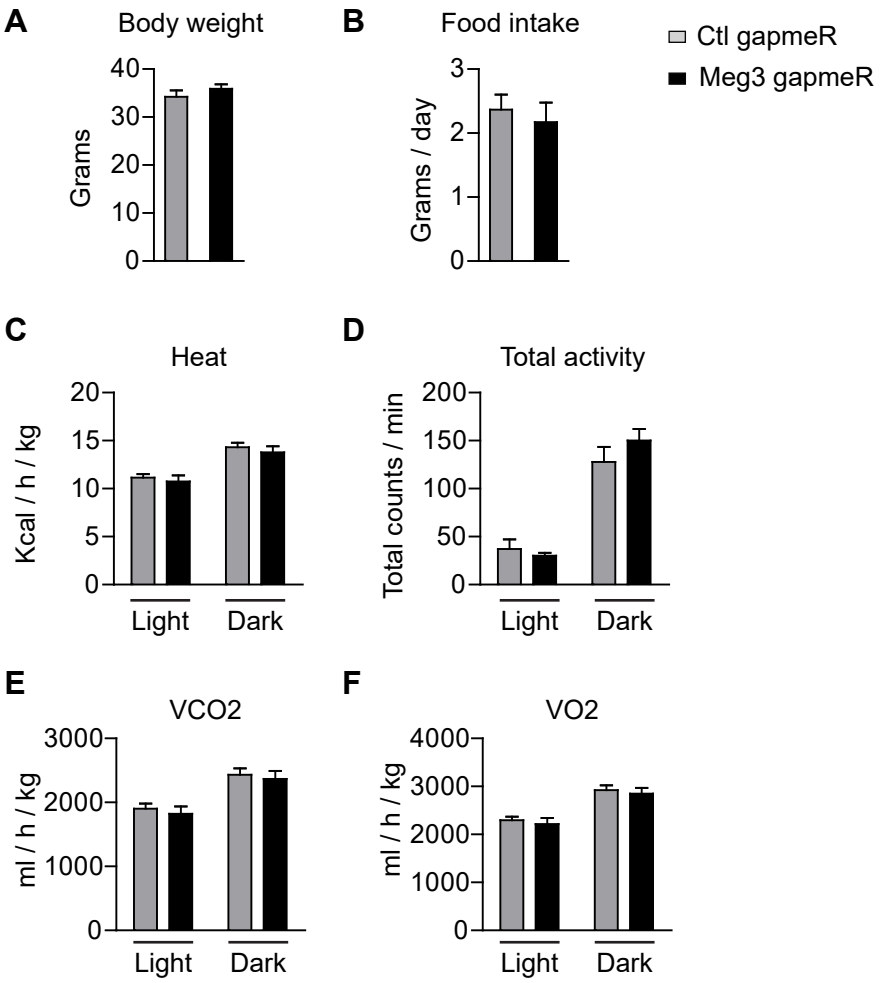

Fig. S4. Metabolic cage studies. Meg3 knockdown (KD) does not affect food intake (A), body weight (B), activities (C), heat (D), CO2 production (E), or oxygen consumption (F) in obese mice. Mean ± SEM, n = 6 mice per group.

Figure S5

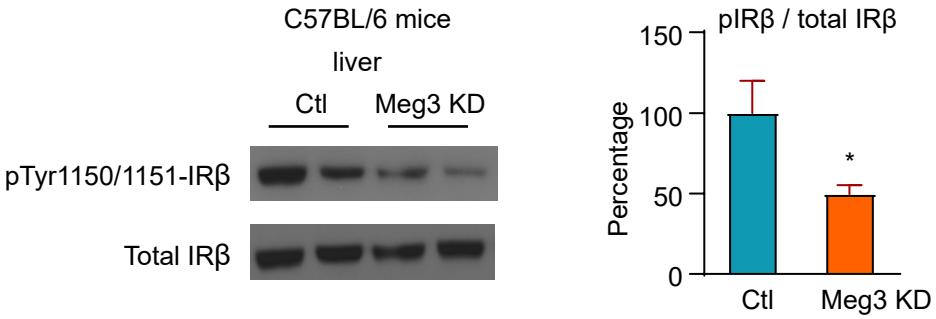

Fig. S5. Meg3 knockdown (KD) reduces the levels of phosphorylated insulin receptor β subunit (IRβ) at Tyr1150/1151. C57BL/6 mice were fed a HFD. At Week 5 on HFD, mice were intravenously injected with control gapmeRs or Meg3 gapmeRs once a week and maintained on HFD up to 12 weeks. Total insulin receptor β and the phosphorylation at Tyr1150/1151 were examined by western blot in the livers of overnight-fasted mice. The tissues were collected at 10 min after insulin injection (0.75 units/kg). Values are mean ± SEM, n = 4 per group; *, $P < 0.05$.

Figure S6

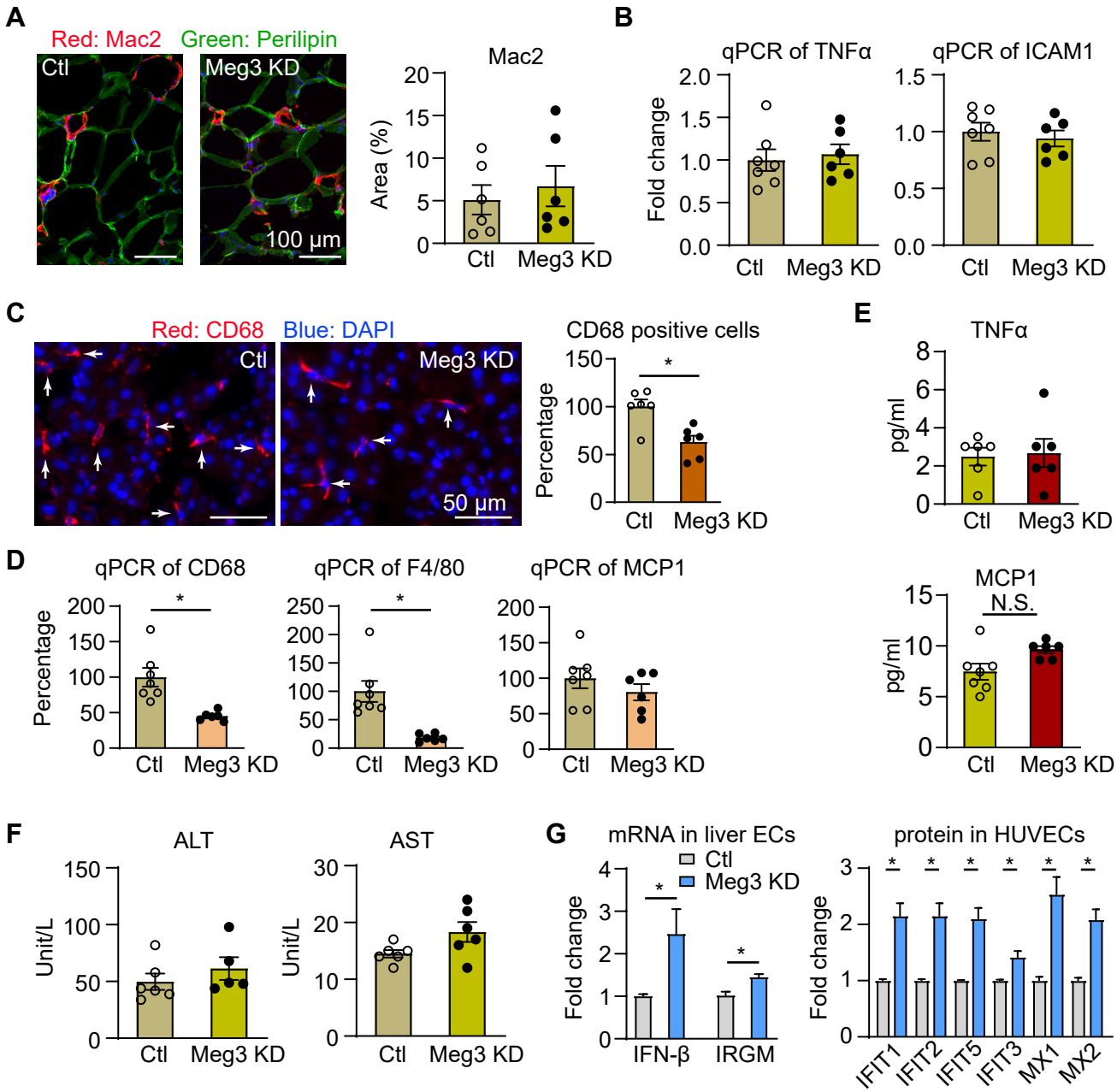

Fig. S6. Meg3 knockdown (KD) does not increase systemic inflammation in obese mice. **(A-F)** C57BL/6 mice were fed on a HFD and treated with control gapmeRs or Meg3 gapmeRs (n = 6 or 7 mice per group). **(A)** Immunofluorescence staining of Mac2 (macrophage marker) and perilipin (adipocyte marker) on eWATs sections and Mac2 quantification. **(B)** The expression of inflammatory genes was examined in eWATs by qPCR. **(C)** Immunofluorescence staining and quantification of CD68 (macrophage marker) on liver sections. **(D)** The expression of CD68 and F4/80 (macrophage markers) and MCP1 (chemokine) was examined in livers by qPCR. **(E)** The levels of plasma TNFα and MCP1 were analyzed by ELISA. **(F)** Plasma levels of ALT and AST were examined in mice treated with control gapmeRs or Meg3 gapmeRs. **(G)** Meg3 knockdown induces type I interferon response in hepatic endothelium (n=6 or 7) and in HUVECs (n=3). For all panels, values are mean ± SEM; *, $P < 0.05$.

Figure S7

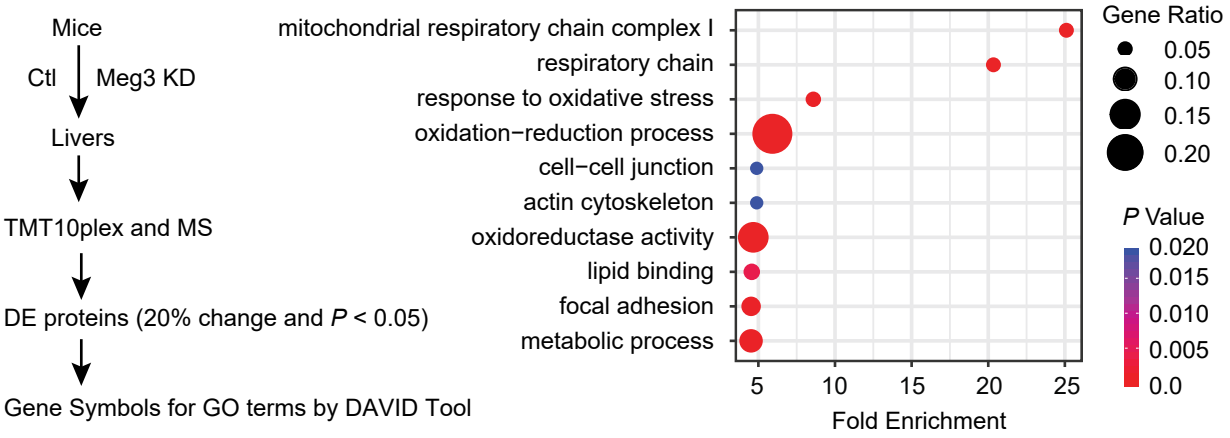

Fig. S7. The top ten GO terms that regulated by Meg3. Livers of obese mice injected with control gapmeRs or Meg3 gapmeRs (Meg3 KD) were subjected to quantitative proteomics (TMT10plex labeling and mass spectrometry) and bioinformatics analysis of genes encoding differentially expressed proteins.

Figure S8

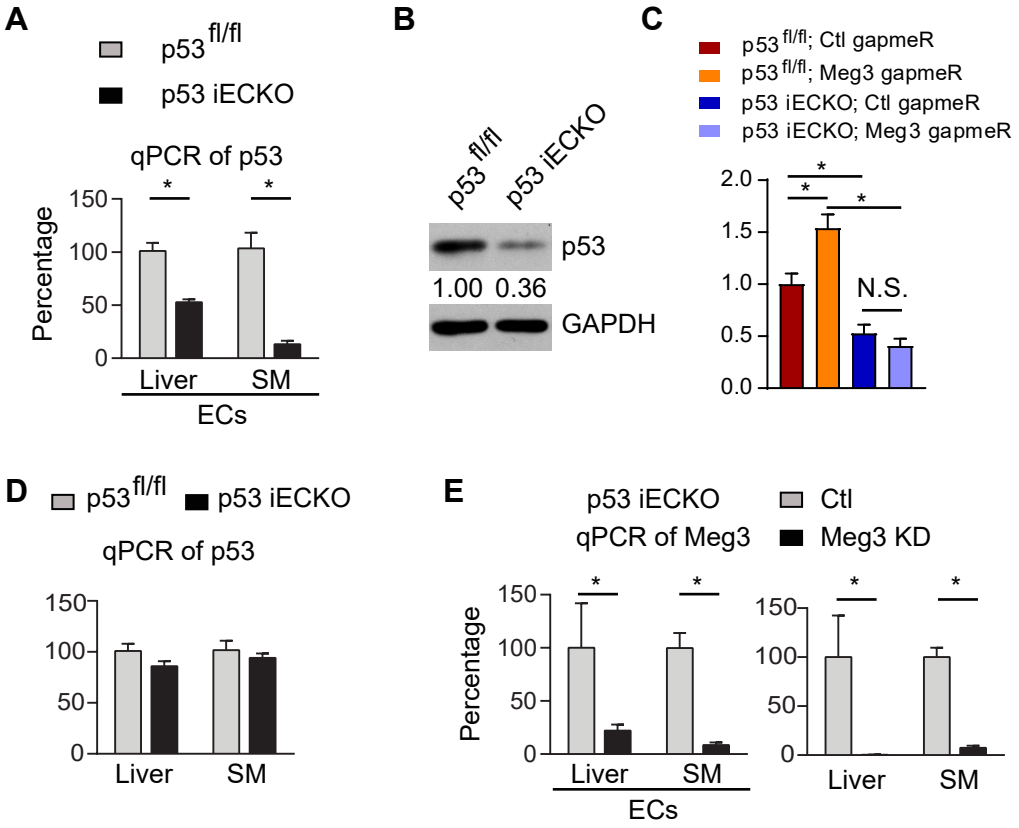

Fig. S8. p53 and Meg3 expression in the freshly isolated ECs or in the indicated tissues by qPCR or western blot. **(A)** p53 expression was examined in the freshly isolated ECs of livers and skeletal muscles (SM) by qPCR (n = 5 for p53 floxed mice; n=14 for p53 iECKO mice). **(B)** p53 expression was examined in the freshly isolated liver ECs by western blot. ECs were pooled from three mice each group. **(C)** The expression of CDKN1A was examined in the freshly isolated liver ECs by qPCR (n = 5, 5, 14, 14 for each group of the indicated mice, respectively). N.S., non-significant. **(D)** p53 expression was examined in the livers and skeletal muscles (SM) tissues by qPCR (n = 5 for p53 floxed mice; n=14 for p53 iECKO mice). **(E)** Meg3 expression was examined in the freshly isolated ECs of livers and skeletal muscles (SM) of p53 iECKO mice or in livers and skeletal muscles tissues of p53 iECKO mice (n=7 per group). For all panels, values are mean ± SEM; *, $P < 0.05$.

Figure S9

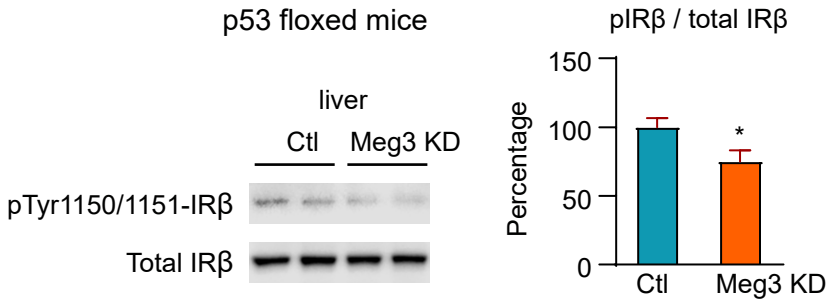

Fig. S9. Meg3 knockdown (KD) reduces the levels of phosphorylated insulin receptor β subunit (IRβ) at Tyr1150/1151. p53 floxed mice were fed a HFD. At Week 5 on HFD, mice were intravenously injected with control gapmeRs or Meg3 gapmeRs once a week and maintained on HFD up to 12 weeks. Total insulin receptor β and the phosphorylation at Tyr1150/1151 were examined by western blot in the livers of overnight-fasted mice. The tissues were collected at 10 min after insulin injection (0.75 units/kg). Values are mean ± SEM, n = 8-12 per group; *, $P < 0.05$.

Supplementary Table S1

Gene	Sequences (5’-3’)
mMeg3 F	TCACCTCCAATTTCCCCTCC
mMeg3 R	GCAAGCCAAGCCTTAAACCT
mCDKN1A F	CCTGGTGATGTCCGACCTG
mCDKN1A R	CCATGAGCGCATCGCAATC
mCDKN2A F	CGCAGGTTCTTGGTCACTGT
mCDKN2A R	TGTTCACGAAAGCCAGAGCG
mGADD45A F	CCGAAAGGATGGACACGGTG
mGADD45A R	TTATCGGGGTCTACGTTGAGC
mRRAD F	GTCAGAGGAGGGCGTTTACAAA
mRRAD R	TCCACAGTGATAGAACGGTCA
hMeg3 F	GGGCATTAAGCCCTGACCTT
hMeg3 R	CCTTGGGGAGGGAAACACTC
hCDKN1A F	CTGGAGACTCTCAGGGTCGAAA
hCDKN1A R	GATTAGGGCTTCCTCTTGGAGAA
hCDKN2A F	GGGTTTTCGTGGTTCACATCC
hCDKN2A R	CTAGACGCTGGCTCCTCAGTA
hGAPDH F	ATGGGGAAGGTGAAGGTCG
hGAPDH R	GGGGTCATTGATGGCAACAATA
mTNFα F	CCCTCACACTCAGATCATCTTCT
mTNFα R	GCTACGACGTGGGCTACAG
mICAM1 F	GTGATGCTCAGGTATCCATCCA
mICAM1 R	CACAGTTCTCAAAGCACAGCG
mCD68 F	TGTCTGATCTTGCTAGGACCG
mCD68 R	GAGAGTAACGGCCTTTTTGTGA
mF4/80 F	CCCCAGTGTCCTTACAGAGTG
mF4/80 R	GTGCCCAGAGTGGATGTCT
mMCP1 F	TTAAAAACCTGGATCGGAACCAA
mMCP1 R	GCATTAGCTTCAGATTTACGGGT
mIFN-β F	GCACTGGGTGGAATGAGACT
mIFN-β R	AGTGGAGAGCAGTTGAGGACA
mIRGM F	CATAGGGAACTTCTGCCGGA
mIRGM R	AGTTGGTTCCTTCGAATGCCT
mp53 F	CCATGGCCCCTGTCATCTTT
mp53 R	TGAGGGGAGGAGAGTACGTG
mHprt F	TCAGTCAACGGGGGACATAAA
mHprt R	GGGGCTGTACTGCTTAACCAG

Supplementary Table S2. Biometrics of human subjects

Group	*n*	M / F	Age (year)
Normal	7	5 / 2	42 ± 16
NAFLD	6	2 / 4	48 ± 20
NASH	7	0 / 7	55 ± 10

Supplementary Table S3

	Identified Proteins	Gene Name	MW	Expression
1	Major urinary protein 1	Mup1	21 kDa	Down
2	Major urinary protein 10	Mup10	21 kDa	Down
3	FERM, RhoGEF and pleckstrin domain-containing protein 1	Farp1	119 kDa	Down
4	NADPH oxidase organizer 1	Noxo1	39 kDa	Down
5	E3 ubiquitin-protein ligase NEDD4	Nedd4	103 kDa	Down
6	Aldose reductase-related protein 2	Akr1b8	36 kDa	Down
7	Plexin-B2	Plxnb2	206 kDa	Down
8	A-kinase anchor protein 13	Akap13	304 kDa	Down
9	Lipoma-preferred partner homolog	Lpp	66 kDa	Down
10	CMRF35-like molecule 9	Cd300lg	37 kDa	Down
11	Beta-1-syntrophin	Sntb1	58 kDa	Down
12	CD166 antigen	Alcam	65 kDa	Down
13	Membrane associated guanylate kinase, WW and PDZ domain containing 3	Magi3	162 kDa	Down
14	Propionyl-CoA carboxylase alpha chain, mitochondrial	Pcca	80 kDa	Down
15	Protein kinase C and casein kinase II substrate protein 3	Pacsin3	49 kDa	Down
16	Betaine--homocysteine S-methyltransferase 1	Bhmt	45 kDa	Down
17	Gephyrin OS=Mus musculus	Gphn	84 kDa	Down
18	Cysteine-rich protein 2	Crip2	23 kDa	Down
19	Succinate--hydroxymethylglutarate CoA-transferase	Sugct	48 kDa	Down
20	CASP8-associated protein 2	Casp8ap2	219 kDa	Down
21	Myb-binding protein 1A	Mybbp1a	152 kDa	Down
22	Non-histone chromosomal protein HMG-14	Hmgn1	9 kDa	Down
23	Methylcytosine dioxygenase TET3	Tet3	180 kDa	Down
24	Sulfotransferase	Sult1a1	30 kDa	Down
25	Mitochondrial peptide methionine sulfoxide reductase	Msra	26 kDa	Down
26	Alpha-defensin 20	Defa20	11 kDa	Down
27	Diphosphomevalonate decarboxylase	Mvd	44 kDa	Down
28	Propionyl-CoA carboxylase beta chain, mitochondrial	Pccb	58 kDa	Down
29	Carnitine O-palmitoyltransferase 2, mitochondrial	Cpt2	74 kDa	Down
30	Tetratricopeptide repeat protein 36	Ttc36	20 kDa	Down
31	Partner of Y14 and mago	Pym1	23 kDa	Down

32	Citrate lyase subunit beta-like protein, mitochondrial	Clybl	38 kDa	Down
33	Alpha-tocopherol transfer protein	Ttpa	32 kDa	Down
34	Oxysterol-binding protein-related protein 2	Osbpl2	55 kDa	Down
35	Talin-2	Tln2	272 kDa	Down
36	Mitochondrial antiviral-signaling protein	Mavs	53 kDa	Down
37	Epidermal growth factor receptor substrate 15	Eps15	98 kDa	Down
38	Histone H1.0	H1f0	21 kDa	Down
39	EH domain-containing protein 3	Ehd3	61 kDa	Down
40	N(G),N(G)-dimethylarginine dimethylaminohydrolase 1	Ddah1	31 kDa	Down
41	Thyroid hormone-inducible hepatic protein	Thrsp	17 kDa	Down
42	Cytosolic non-specific dipeptidase	Cndp2	53 kDa	Down
43	Alpha-actinin-4	Actn4	105 kDa	Down
44	Intracellular hyaluronan-binding protein 4	Habp4	46 kDa	Down
1	Nidogen-1	Nid1	137 kDa	up
2	Polymerase I and transcript release factor	Ptrf	44 kDa	up
3	NADH dehydrogenase [ubiquinone] 1 alpha subcomplex subunit 12	Ndufa12	18 kDa	up
4	Eukaryotic translation initiation factor 3 subunit C	Eif3c	106 kDa	up
5	Carbonic anhydrase 3	Ca3	29 kDa	up
6	Apolipoprotein E	Apoe	36 kDa	up
7	NADH dehydrogenase [ubiquinone] iron-sulfur protein 2, mitochondrial	Ndufs2	50 kDa	up
8	L-serine dehydratase/L-threonine deaminase	Sds	35 kDa	up
9	Flavin reductase (NADPH)	Blvrb	22 kDa	up
10	Transcriptional activator protein Pur-alpha	Pura	35 kDa	up
11	Hydroxyproline dehydrogenase	Prodh2	51 kDa	up
12	Alanyl-tRNA editing protein Aarsd1	Aarsd1	45 kDa	up
13	Isobutyryl-CoA dehydrogenase, mitochondrial	Acad8	45 kDa	up
14	Glutathione S-transferase omega-1	Gsto1	27 kDa	up
15	Alanine aminotransferase 2	Gpt2	58 kDa	up
16	Methyltransferase-like protein 7B	Mettl7b	28 kDa	up
17	NADH dehydrogenase [ubiquinone] iron-sulfur protein 8, mitochondrial	Ndufs8	24 kDa	up
18	Fructose-1,6-bisphosphatase 1	Fbp1	37 kDa	up
19	Aldehyde dehydrogenase X, mitochondrial	Aldh1b1	58 kDa	up
20	NADH dehydrogenase [ubiquinone] 1 beta subcomplex subunit 10	Ndufb10	21 kDa	up
21	Metastasis-associated protein MTA2	Mta2	75 kDa	up

22	NADH dehydrogenase [ubiquinone] 1 alpha subcomplex subunit 9, mitochondrial	Ndufa9	43 kDa	up
23	Capping protein (Actin filament), gelsolin-like	Capg	39 kDa	up
24	Laminin subunit beta-2	Lamb2	197 kDa	up
25	Sulfurtransferase	Mpst	33 kDa	up
26	Dipeptidyl peptidase 2	Dpp7	56 kDa	up
27	Gamma-butyrobetaine dioxygenase	Bbox1	45 kDa	up
28	NADH dehydrogenase [ubiquinone] 1 beta subcomplex subunit 11, mitochondrial	Ndufb11	17 kDa	up
29	Alcohol dehydrogenase 1	Adh1	40 kDa	up
30	UDP-glucuronosyltransferase	Ugt2b34	61 kDa	up
31	Erythrocyte band 7 integral membrane protein	Stom	31 kDa	up
32	Myristoylated alanine-rich C-kinase substrate	Marcks	30 kDa	up
33	Telomerase protein component 1	Tep1	291 kDa	up
34	3-ketoacyl-CoA thiolase B, peroxisomal	Acaa1b	44 kDa	up
35	Integrin beta-1	Itgb1	88 kDa	up
36	RAB1A, member RAS oncogene family	Rab1a	22 kDa	up
37	High mobility group protein B2	Hmgb2	24 kDa	up
38	Heme oxygenase 2 (Fragment)	Hmox2	26 kDa	up
39	Cathepsin F	Ctsf	52 kDa	up
40	Cytochrome P450 2E1	Cyp2e1	57 kDa	up
41	MCG10343, isoform CRA_b	Slc25a3	40 kDa	up
42	Ras-related protein Rab-1B	Rab1b	22 kDa	up
43	Deoxyuridine triphosphatase	Dut	21 kDa	up
44	Collagen type IV alpha-3-binding protein	Col4a3bp	71 kDa	up
45	Indolethylamine N-methyltransferase	Inmt	29 kDa	up
46	Alcohol dehydrogenase 4	Adh4	40 kDa	up
47	Chloride intracellular channel protein 4	Clic4	29 kDa	up
48	Histone H1.5	Hist1h1b	23 kDa	up
49	Bile acyl-CoA synthetase	Slc27a5	76 kDa	up
50	Collagen alpha-1(XIV) chain	Col14a1	193 kDa	up
51	Histone H1.3	Hist1h1d	22 kDa	up
52	Ferritin	Ftl1	21 kDa	up
53	Carboxylesterase 1E	Ces1e	62 kDa	up
54	Glutathione S-transferase A4	Gsta4	26 kDa	up
55	Ferritin heavy chain	Fth1	21 kDa	up

56	Coronin-1A	Coro1a	51 kDa	up
57	Ear6 protein	Ear6	17 kDa	up
58	Heat shock protein beta-1	Hspb1	23 kDa	up
59	Adenylate kinase 2, mitochondrial (Fragment)	Ak2	7 kDa	up
60	Epoxide hydrolase	Ephx1	51 kDa	up